We are IntechOpen, the world's leading publisher of Open Access books Built by scientists, for scientists

4,800
Open access books available

122,000
International authors and editors

135M
Downloads

Our authors are among the

154
Countries delivered to

TOP 1%
most cited scientists

12.2%
Contributors from top 500 universities

CLARIVATE ANALYTICS BOOK CITATION INDEX INDEXED

WEB OF SCIENCE™

Selection of our books indexed in the Book Citation Index in Web of Science™ Core Collection (BKCI)

Interested in publishing with us?
Contact book.department@intechopen.com

Numbers displayed above are based on latest data collected.
For more information visit www.intechopen.com

14

Micro/nano scale phase front inscription on polymer thin layer for flexible beam shaping

Jun Ki Kim[1] and Kyunghwan Oh[2]
[1]*Harvard medical school,*
Massachusetts General Hospital
U.S.A
[2]*Yonsei University, Department of Physics,*
Republic of Korea

1. Introduction

As the demands for non-spherical lenses or diffractive optical devices have been increased, much investigation efforts over Beam transforming and the wavefront control in optical technologies have been attempted. Thus, novel and various technologies have been proposed in order to transform the shape and power distribution of a given light beam. Through waveguide-branching or phase front matching methods which were previously reported, the controlling of either phase front curvature or power distributions had been achieved. However, beam reshaping technique using these methods relied mainly on the use of bulk optical system, which required complicated design and fabrication processes at the risk of system size as well as cost.

Along with fast development in fiber optic communications and sensory systems, various attempts in order to cope with these weaknesses have been made to incorporate the bulk-optic technique into optical fibers. Direct mechanical deformation of fiber ends into spherical or wedge-shaped surfaces have been attempted as one of first attempt in fiber optics for applications in laser-diode to optical fiber coupling. By utilizing conventional micro-lithography and etching techniques, reflowing technique of photoresist on the fiber ends have been also attempted. However, laser direct writing process over optical fiber endfaces suffers from not only sophisticated optical alignments and expensive femto-second laser systems but also surface damages after fabrication process.

Recently, the polymeric phase-front modification technique using optical fiber composition was investigated by the authors in order to overcome the disadvantages of described methods. As the proposed methods are suitable for beam forming and beam pattern control in the fiber optic system, it was confirmed that the device showed strong potentials for flexible and economic optical phase-front control without resorting to conventional lithography and etching techniques.

Thus, in this chapter, micro/nano scale phase front inscription techniques were introduced and investigated for flexible beam shaping on polymer thin layer. The numerical simulation of the diffraction patters out of azo-polymer layer on the fiber was analyzed. In parallel, a

new method to inscribe linear and concentric circular surface relief gratings (SRGs) to manipulate the propagation properties of a beam was described. The principles, fabrication procedure, and characterization of beam propagation and beam patterns from linear and circular azo-polymer SRGs are discussed both experimentally and theoretically.

2. Formation of surface relief grating (SRG) on Azo polymer thin layer

2.1 Azobenzene-functionalized polymers

Azo-polymer complexes having unique mass shift property induced by photo-reaction have been widely used for inscribing of the periodic optical structures. Thus, there have been many reports that use them to generate spontaneous surface modulation by exposing different light intensity on an Azo-polymer thin film. In essence, the polymer material will reversibly deform so as to minimize the amount of material exposed to the light. This phenomenon is not a kind of laser ablation, since it readily occurs at low power as well as the transformation is reversible. Although this is clearly related to the azobenzene isomerization, the exact mechanism of this phenomenon is still unresolved.

Azoxy has a double bond group of atom. Especially, it has a double bond of Nitrogen in the both terminal of the molecular formula as shown in Figure 1 as chemical structures.

The epoxy-based azo polymer PDO3 was synthesized from diglycidyl ether of bisphenol A and 4-(4′-nitrophenylazo) phenyl amine for the investigations. The *Tg*s of the azo polymers are about 106 °C for PDO3. Figure 2 shows the UV–visible absorption spectra of the azo films. As the absorption band of the azo-polymer is in the range of blue-green band, Ar-ion laser source is generally utilized as an inscribing laser beam.

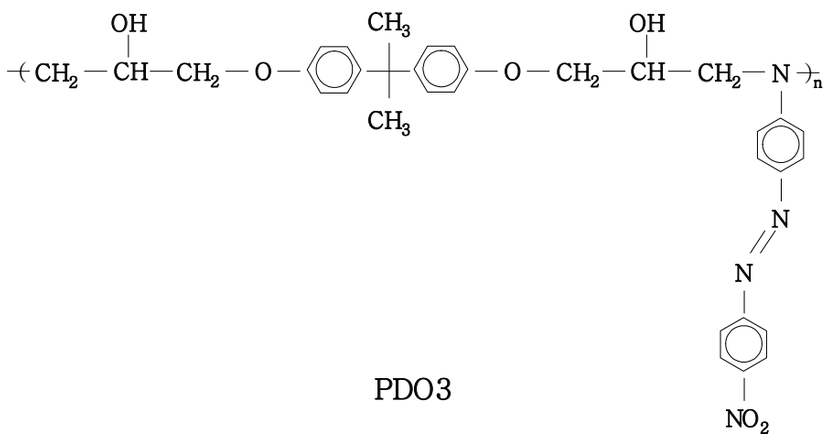

PDO3

Fig. 1. The chemical structures of PDO3

Typical surface deformation images of Azo-polymer under various engraving conditions are shown in Figure 3. Figure 3(a) depicts modulated surface induced by one-dimensional Gaussian beam, and Figure 3(b) and 3(c) show the typical surface deformation induced by the linearly and circularly polarized Gaussian beams, respectively. The engraved diameter and the modulation depth are dependent upon engraving conditions such as polarization condition, launched laser power, laser beam diameter and exposure time.

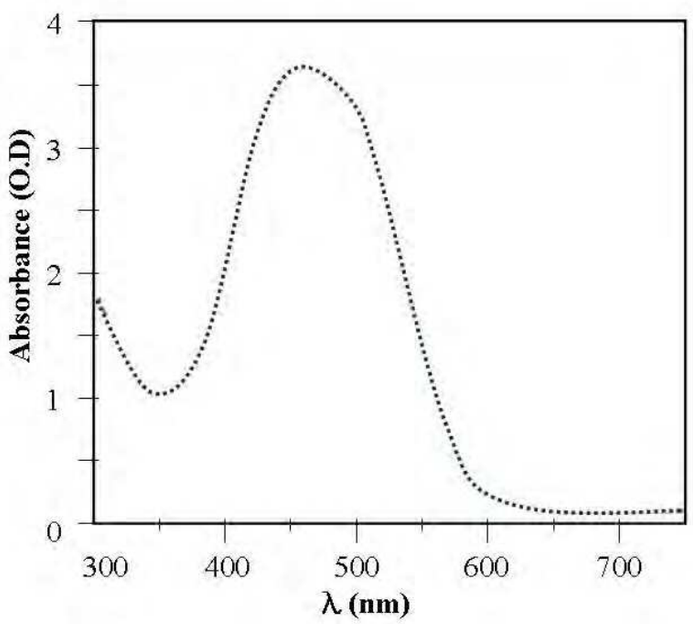

Fig. 2. Absorbance of azopolymer

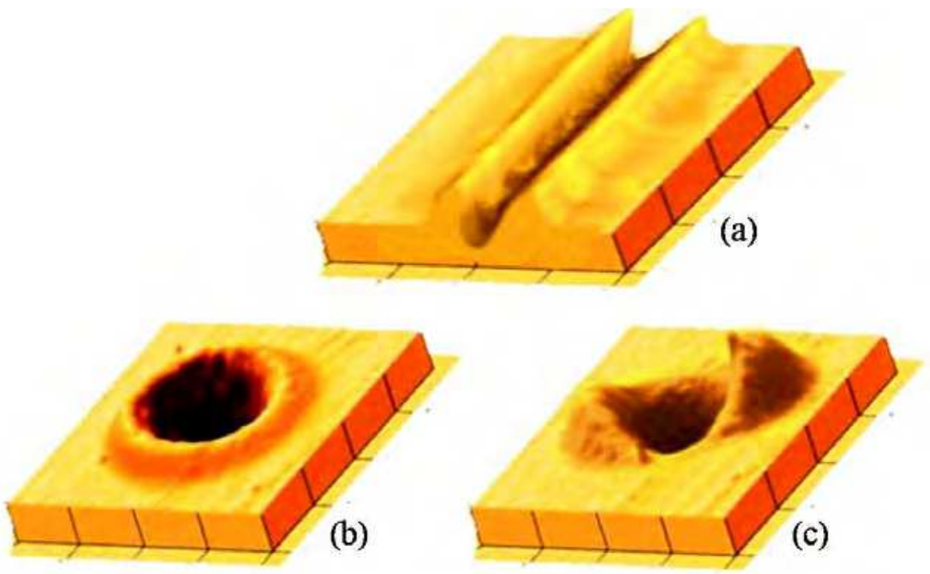

Fig. 3. Typical surface deformation images of Azo polymer induced by Gaussian beam

Table 1 describes the diffraction efficiencies and surface modulation of the gratings which are recorded under different recording conditions. The different polarizations defined by an angle α, with respect to *s* polarization.

In comparison with photoresist films, Azo-polymer layers produce surface relief grating (SRG) pattern by absorption of blue-green photons, where the actual mass of layer is modulated rather than refractive index. In a single-step writing process, topographic structures on the azo-polymer layers can be formed upon exposure to the appropriate

optical patterns. This process, therefore, has a significant advantage over other techniques which typically require complicate process, such as baking, exposure and developing, etc.

Recording conditions	Difraction efficiency (%)	Surface modulation (Å)
α = 0˚	<0.01	<100
α =16˚	5.5	1470
α =45˚	27	3600
α =90˚	15.2	2540
Unpolarized	16.5	2560
Circularly polarized	30	3500

Table 1. The diffraction efficiencies and surface modulations under different recording conditions.

2.2 Formation of linear and circular pattern

Most significant merit for developing interferometric lithography on optical fibers is that both linear and concentric phase-fronts over the azo-polymer layers could be inscribed in a single exposure without using any photo-mask, or further post-processes. For the linear SRGs, linear fringe patterns were generated by using conventional two-beam interference set-up based on bulk-optics. In contrast to these linear SRGs, compact fiber-optic pattern generation method was utilized in the circular SRGs. The concentric interference pattern was generated within the cross section of the fiber, using a coreless fiber segment and adjusting its length.

In both linear and concentric SRGs, three main steps for preparing a sample are required; Azo-polymer thin film coating on fiber end facet, and optical interference pattern generation and exposure to the inscribing laser beam. It is noteworthy that these one-step and direct exposure methods of various phase-fronts over optical fiber could provide strong economical mass production capability to the both fiber array and planar waveguides.

An optical fiber was, firstly, cleaved to form an optically flat endface, which makes a right angle with respect to the fiber axial direction, using an ultrasonic high precision fiber cleaver. The cleaved endface served as a substrate for azo polymer thin film coating. PDO3 polymer containing azo-benzene group was solvated in cyclohexanone and the filtered 10wt% PDO3 solution was dropped on the fiber-end-surface and then spin-coated. The film was, then, dried in a vacuum oven at 80°C for 1-hour. Thin film layer of azo-polymer with flat and smooth surface could be possible due to relatively low viscosity of the solution. The thickness of the thin film layer was 900nm having a flatness of ±20nm over the entire circular optical fiber endface.

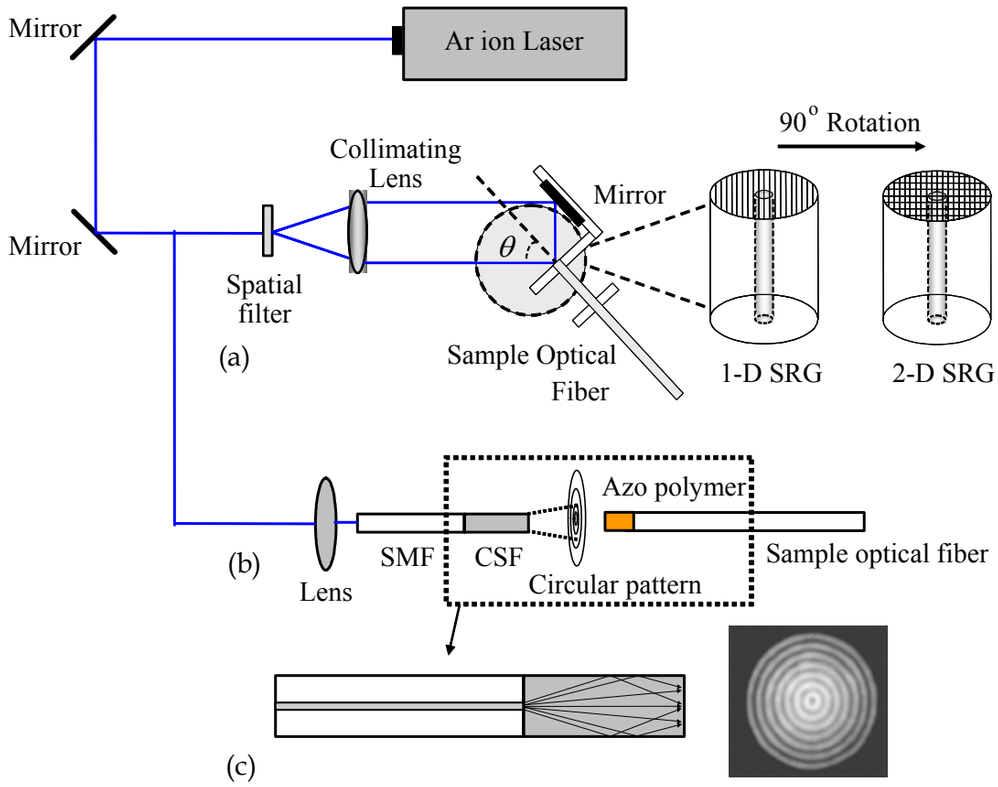

Fig. 4. Experimental setup

Generation for optical interference pattern and exposure process is shown in Figure 4. It is notable that the proposed process is direct one-step exposure to generate SRGs obviating photo masks and etching processes for both linear, (a), and concentric, (b), (c). Schematic diagram for fabrication of linear SRGs is presented in Figure 4-(a). An Ar-ion laser was used as a writing beam. The laser beam intensity was 100 mW/cm² and operating wavelength was 488nm which is in the range of absorption band of the azo-polymer. The laser beam was expanded by a spatial filter and collimated by a collimator. Linear interference patterns were formed due to optical path difference between the direct beam and reflected beam at the mirror. The pitch of interference was adjusted by changing the incident angle θ, which determined the period (Λ) of SRG pattern on azo-polymer film. The incident angle was adjusted to 7° in order to inscribe a uniform linear pattern with a pitch of 2μm. Once the linear interference pattern was exposed to azo-polymer, 1-dimensional SRG was formed by the mass-shift. After adjusting the alignment of the fiber at an angle of 90°, another pattern can be superimposed to form a 2-dimensional SRG. After this double exposure process, a well-defined 2D grating was fabricated.

The schematic diagrams for concentric SRGs pattern generations are shown in Fig 4-(b), and (c). The pattern generation method for concentric interference is based on a compact all-optical fiber device, which is contrast to the linear SRGs based on conventional bulk optics in Fig 4-(a). The device was composed of conventional single mode fiber (SMF) and coreless silica fiber (CSF) without GeO_2 doped core. The LP01 mode exits from the SMF core and it

passes through CSF with expanding the beam diameter, which can be approximated by Gaussian beam propagation.
As the beam further propagates along CSF, part of the beam hits the air-glass interface, and then reflects into CSF, generating circular interference patterns. The schematic diagrams for concentric SRGs pattern generations are shown in Fig 4-(b), and (c). The pattern generation method for concentric interference is based on a compact all-optical fiber device, which is contrast to the linear SRGs based on conventional bulk optics in Fig 4-(a). The device was composed of conventional single mode fiber (SMF) and coreless silica fiber (CSF) without GeO2 doped core. The LP01 mode exits from the SMF core and it passes through CSF with expanding the beam diameter, which can be approximated by Gaussian beam propagation.

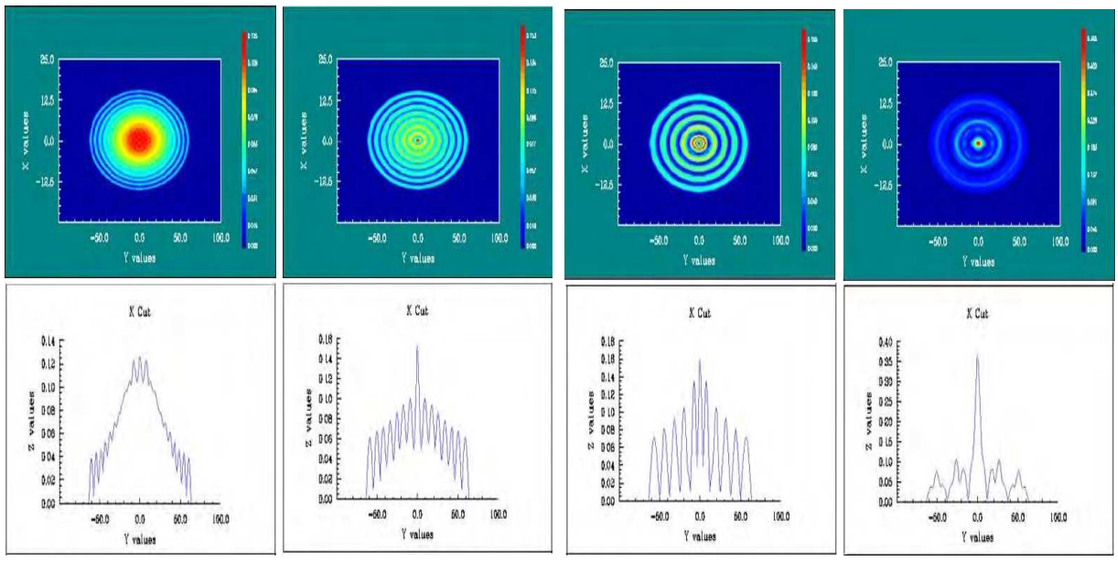

(a) L=700μm **(b) L=1000μm** **(c) L=1500μm** **(d) L=3000μm**

Fig. 5. The numerical estimation of the intensity distributions

In order to further investigate the concentric interference pattern generation in terms of variation of CSF lengths, a commercial beam propagation method (BPM) package, BeamPROP™, was utilized for numerical analysis. The results are summarized in Figure 5. Here we assumed the fundamental mode of SMF can be approximated as a Gaussian beam as it propagates along CSF, which has been widely accepted for calculation of light propagation in the free space out of SMF. The outer diameter of both SMF and CSF were 125μm. The intensity profile and fringe spacing at the surface of CSF were directly dependent on the CSF length for the given diameter as shown in Figure 5. Gaussian distribution profile without concentric fringes is maintained under the condition of CSF length less than 700μm. As the CSF length approaches near 700μm, fringe patterns appear overlaid on the Gaussian beam. For CSF length longer than 900μm, the entire cross-section of CSF is filled with concentric interference fringes. As the CSF length increases furthermore, less numbers of fringes and longer pitch were predicted. Furthermore, by varying the distance between the CSF end face and azo-polymer end face, the fringe spaces could be

adjustable. Therefore, the proposed composite fiber-optic device can provide very versatile and flexible control over the concentric interference pattern generation, by varying the geometrical dimension of CSF, diameter and segment length.

2.3 Surface relief grating (SRG) on optical fiber surface

The scanning electron microscope (SEM) images and blow up images of the fabricated SRGs are shown in Figure 6. One and Two-dimensional linear SRG are shown in Figure 6-(a) and (b), respectively. The bright center regions of the figures denote the location of the fiber core. Firstly, one-dimensional (1-D) linear SRG was fabricated on the fiber-end-surface. The pitch was 2μm and the modulation depth was in the range of 450~500nm. For this 1-D SRG, another linear interference pattern was exposed after rotating the fiber at an angle of 90 degrees from the initial position, to form two-dimensional (2-D) linear SRGs as in Figure 4-(a). As a result, periodic 2-D SRG patterns with 2μm -by-2μm were engraved on the target surface shown in Figure 6(b). Through the SRG pattern, the fundamental mode guided by the SMF spreads out to the entire cross section of the engraved facet and derives effective modification of the phase front of incident beam on it.

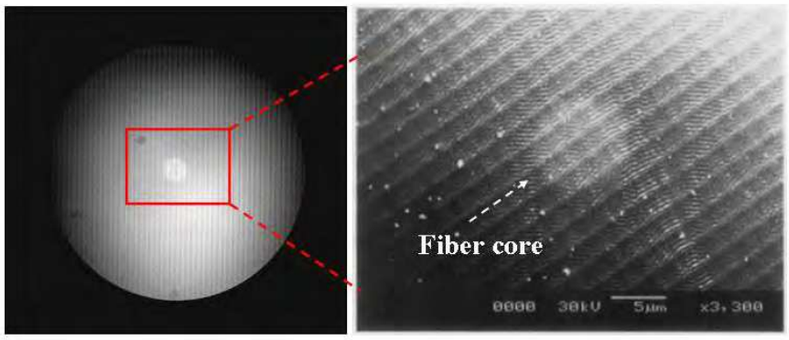

(a)

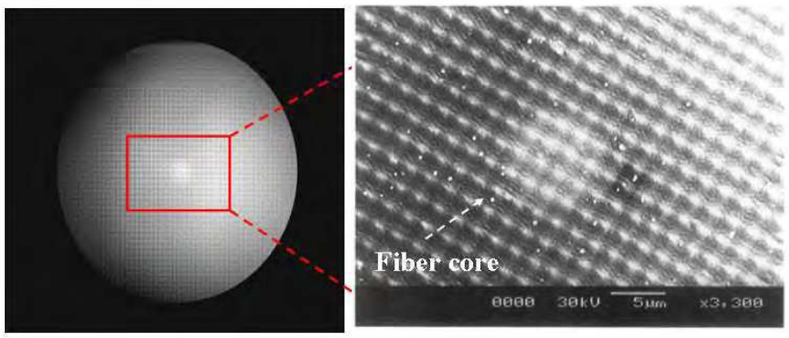

(b)

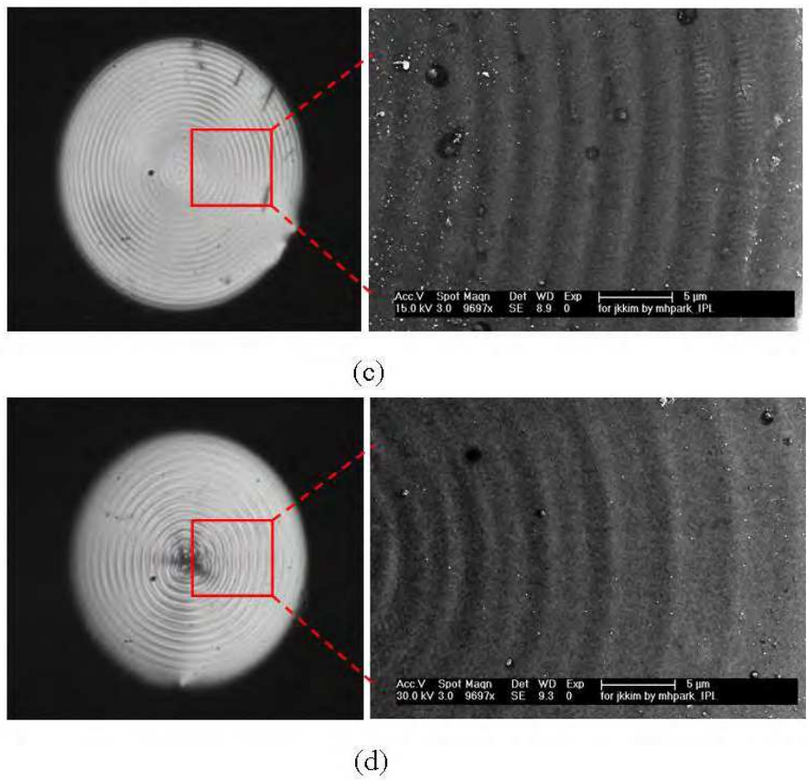

Fig. 6. SEM images on the fiber-end-surface with 1-D/2-D linear and concentric SRG

In concentric SRGs, on the while, the composite SMF-CSF pattern generators with the CSF lengths of 1000µm and 1500µm was used, and the SEM images of fabricated SRGs are shown in Figure 6(c) and (d), respectively. The pitches of the engraved concentric SRG patterns were about 2.7 and 4.3µm for Figure 6(c) and (d), respectively. The concentric pattern generation using all-optical fiber device shows same concentric SRG properties, as numerically predicted in Figure 5. Thus, it was experimentally confirmed that direct exposure of both linear and concentric interference pattern at 488nm Ar-ion laser can successfully form the corresponding SRGs by using azo-polymer thin films over SMFs.

3. Measurements and simulations

3.1 Measurements of diffraction patterns out of SRGs

The optical field propagating through the SMF will experiences the spatially periodic modulation provided by the SRGs at the prepared endface of the fiber, resulting in unique diffraction patterns. Fabricated SRGs on SMF were further examined in terms of their diffraction pattern both experimentally and theoretically. In order to investigate impact of the SRGs over beam patterns, the far-field diffraction patterns from the SRG on SMFs were measured by a CCD camera using a laser source at 635 nm.

In Figure 7(a), schematic diagram of the experimental setup for measurement of diffraction patterns is shown, where L is the distance from the SRG to the measured diffraction patterns, and D is the distance between the 0th and the 1st order diffraction beam pattern, and θ_m is the diffraction angle. From the diffraction patterns, we can calculate the diffraction angle

(θ_m) by measuring the distance data (D and L), and finally obtain the SRG pitch (Λ) from the following diffraction grating equation

$$\Lambda = m\lambda / \sin\theta_m \quad (1)$$

where m denotes the order of principle maxima.

For the case of linear SRGs, measured diffraction patterns and the line profile is shown in Figure 7-(b),(c). In Figure 7-(b),(c), clear diffraction beam pattern of the zero'th and the first order from the 1D/2D linear SRG was observed. The circular pattern at the center regions is identified as the zero'th order and two side lobes correspond to the first order diffraction pattern in Figure 7(b). Similarly, the four first order side lobes perpendicular to one another, was measured as shown in Figure 7(c).

The far field diffractive patterns and the line profiles of the concentric SRGs are shown in the Figure 7 (d),(e). In circular SRGs, the orders of diffraction patterns are dependent upon the CSF lengths of 1000 and 1500μm making different concentric patterns. For the case of CSF length of 1000μm, the diffraction pattern has the central zero'th order and one thin ring, which corresponds to 1'st order. In the case of 1500μm CSF, two rings were clearly dissolved. They correspond to 1'st and 2'nd order diffraction, overlaid with the zero'th order circular pattern. In comparison to diffraction patterns from linear SRGs, as in Figure 7-(b),(c), those from the concentric SRGs do not show clear and definitive images, which is attributed to relatively low contrast in the concentric interference pattern generators. See Figure 5-(b) and (c). Minima of the fringes do have finite intensity and subsequently SRG would have shallow contrast to make the diffraction pattern less definitive.

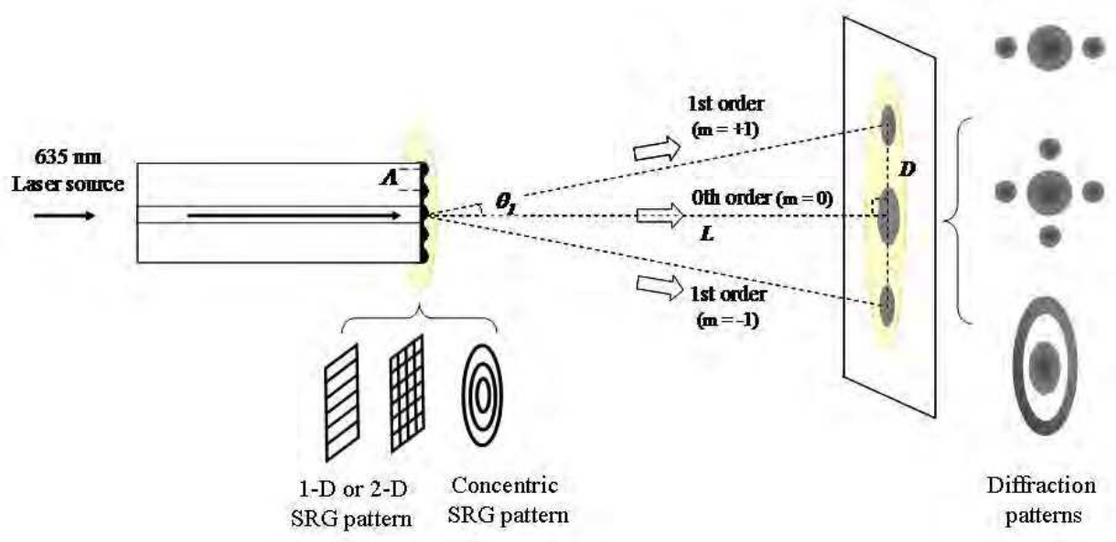

(a)

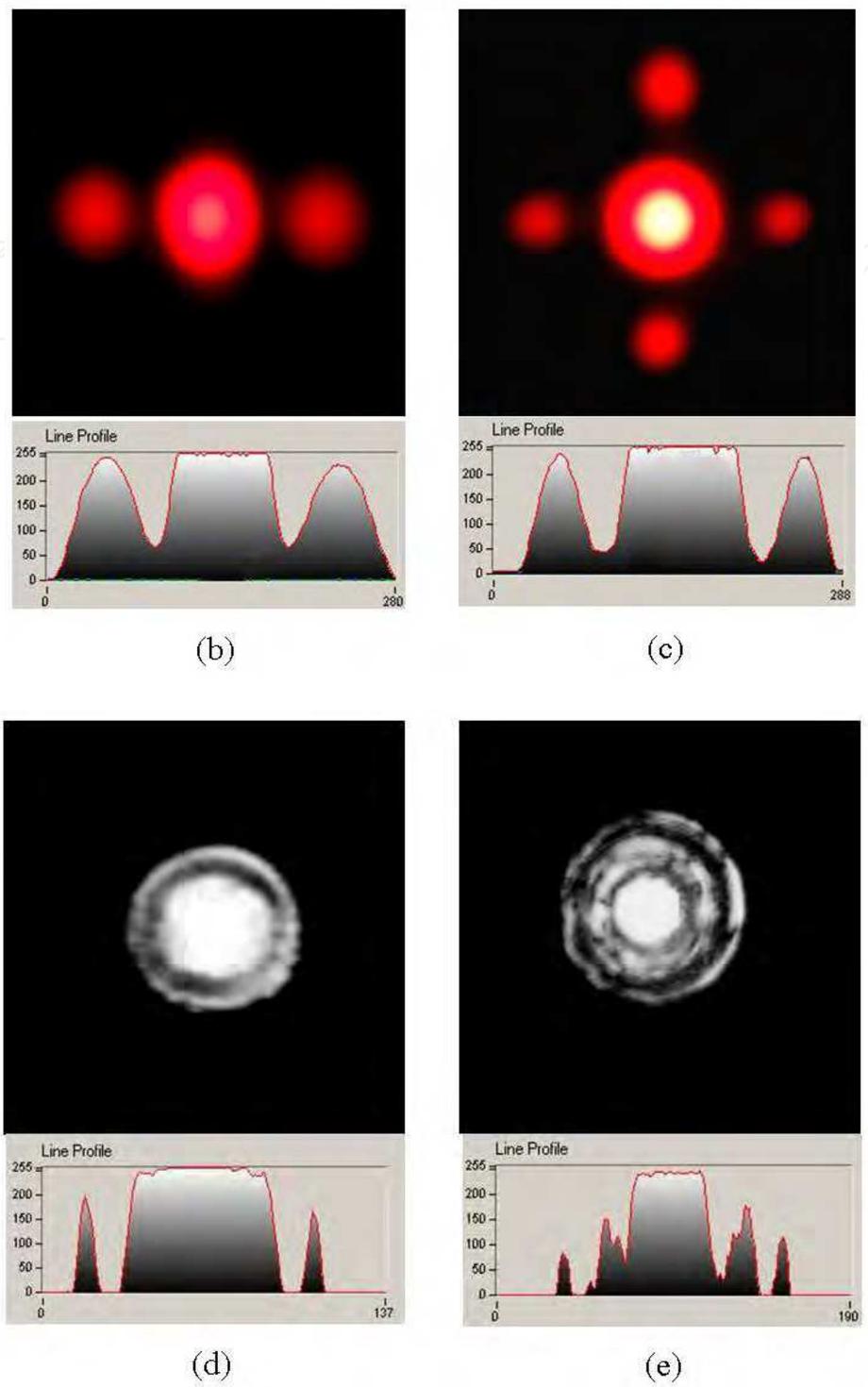

Fig. 7. Schematic diagram for measuring diffraction beam patterns and line profiles

	L [mm]	D [mm]	θ [°]	Λ [μm] (calculated)	Λ [μm] (measured)
1-D SRG	10	3.56	19.60	1.89	2.0
2-D SRG	10	3.39	18.73	1.98	2.0
CSRG with 1000μm	11.68	3.0	14.41	2.55	2.7
CSRG with 1500μm	19.11	3.0	8.92	4.10	4.3

Table 2. Measured data from diffraction pattern measurements

The measured diffraction parameters are shown in Table 2, from which we calculated the pitches (Λ) of SRGs. For linear 1-D/2-D SRGs, pitches were calculated as 1.89μm and 1.98μm, respectively. For concentric SRGs made by the SMF-CSF interference pattern generators of CSF length of 1000 and 1500μm, the pitches were calculated as 2.55 and 4.10μm, respectively. Compared with pitches measured by SEM images in Figure 6 in previous section, these numbers are in a reasonably good agreement as summarized in the last two columns of Table 2.

3.2 Theoretical analysis using simulation tools

Diffraction patterns from the fabricated SRGs on optical fiber endfaces were also theoretically investigated using a commercial simulation package, LightTools™. In the simulation tool, the diffraction of the guided mode from the given SRG was investigated in terms of the irradiance beam patterns using the illumination analysis.

Actual dimension of the SRGs were used in the simulation with an approximation that the incident light is Gaussian, instead of LP_{01} mode of the SMF, which is very common in the free space optic analysis. The illumination analysis in the LightTools is based on a Monte Carlo ray trace. From randomly selected points on the surface or Volume into randomly selected angles in space, it traces the desired number of rays. Diffraction patterns from the linear 2-D SRGs, Figure 6-(b), and concentric SRGs, Figure 6-(c) were simulated and the irradiance chart diagrams are shown in Figure 8. In comparison with experimental measurements, Figure 7-(c) and (d), it was found that the simulation results showed good agreement in terms of the line profiles, the intensity distribution along x or y axis, and diffraction robe locations.

Through these experimental and theoretical analyses, we could confirm that the proposed method to form SRGs on the optical fiber endfaces does have practical feasibility and can endow a new degree of freedom to design integrated optical systems compatible to fiber optics or waveguide optics.

4. Conclusion

By adapting azobenzene polymer layer, both linear and concentric surface relief gratings (SRGs) have been successfully inscribed over optical fiber endfaces based on developing

maskless lithography technology. Utilizing unique advantage of the azo-polymer such as direct writing and multiple exposure capabilities, various SRGs were flexibly designed and fabricated. Two-beam interference patterns were applied for 2-D linear SRGs and SMF-CSF concatenated device was proposed to generate concentric interference patterns for circular SRGs, respectively. Theoretically, the diffraction pattern out of SRGs was investigated by utilizing a Monte Carlo ray tracing package. In comparison with experimental measurement, the simulated results showed good agreement in terms of irradiance beam patterns.
Through the proposed inscription technology based on polymer thin layer coating, micro/nano scale phase front control could be possible for manipulating the propagation properties of the light and it could be applicable in integrated optical components as well as sub-systems for optical communications.

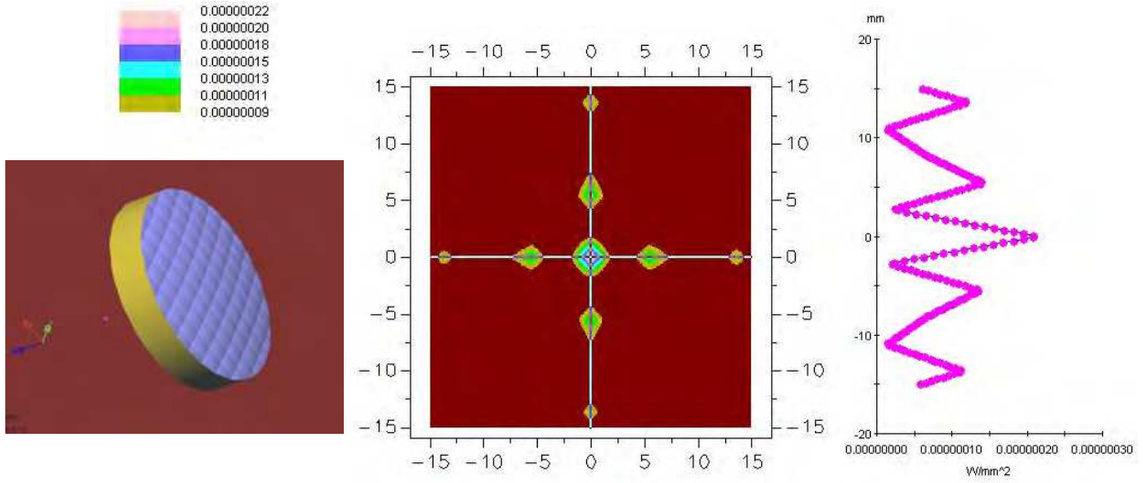

(a)

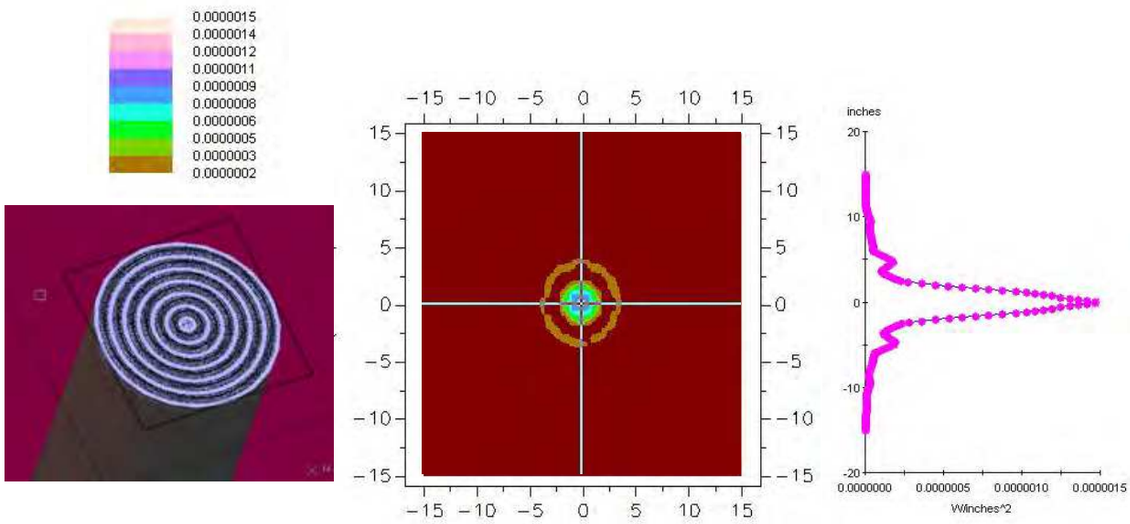

(b)

Fig. 8. The simulation results of the irradiance chart using LightTools™

Acknowledgement
This work was supported by the National Research Foundation of Korea Grant funded by the Korean Government (NRF-2009-352-C00042) and in part by the KOSEF (ROA-2008-000-20054-0, R15-2004-024-00000-0), in part by the KICOS (2009-8-1339, 2008-8-1893), in part by the ITEP (2008-8-1901, 2009-8-0809), and in part by the Brain Korea 21 Project of the KRF

5. References

A. M. Streltsov et al., "Fabrication and analysis of a directional coupler written in glass by nanojoule femtosecond laser pulses.", *Opt. Lett.*, Vol. 26, pp. 42 (2001)

C. J. Barrett, A. L. Natansohn, and P. L. Rochonm, *J. Phys. Chem*. Vol. 100, pp. 8836 (1996)

D. F. Cornwee, "Nonprojective transformation in optics," *Opt. Eng*., Vol. 294, pp. 62-72 (1982)

D. K. Yi et al., "Surface-modulation-controlled three-dimensional colloidal crystals.", *Appl. Phys. Lett.* Vol. 80, pp. 225 (2002)

D. Y. Kim, L. Li, X. L. Jiang, V. Shivshankar, J. Kumar, and S. K. Tripathy, *Macromolecules* 28, pp.8835 (1995)

D. Y. Kim et al., "Laser-induced holographic surface relief gratings on nonlinear optical polymer films.", *Appl. Phys. Lett*., 66, pp. 1166 (1995)

E. Hecht, "Optics," Addison Wesley, San Francisco (2002)

G. Eisenstein and D. Vitello, "Chemically etched conical microlenses for coupling single-mode lasers into single-mode fibers," *Appl. Opt*., Vol. 21, pp. 3470-3474 (1982)

H. Ghafoori-Shiraz and T. Asano, "Microlens for coupling a semiconductor laser to a single-mode fiber," *Opt. Lett*., Vol. 11, pp. 537-539 (1986)

H. Kogelnik, "On the propagation of Gaussian beams of light through lenslike media including those with a loss and gain variation," *Applied Optics*, Vol. 4, pp. 1562 (1965)

H. Rau, in Photochemistry and Photophysics; Vol. 2, edited by J. Rebek (CRC Press, Boca Raton, FL, 1990), pp. 119-141 (1990)

H. Sasaki, "Normalized power transmission in single mode optical branching waveguides," *Electron. Lett*., Vol. 17, pp.136-138 (1981)

Hidehiko Yoda and Kazuo Shiraishi, "A new scheme of a lensed fiber employing a wedge-shaped graded index fiber tip for the coupling between high power laser diodes and single mode fibers," *J. Lightwave Technol*, Vol. 19, pp. 1910 (2001)

J. Kim, M. Han, Selee Chang, W. Lee and K. Oh, "Achievement of large spot size and long collimation length using UV curable self-assembled polymer lens on a beam expanding core-less silica fiber," *IEEE Photonics Technology Letters*, Vol. 16, paper no. 11, pp. 2499-2501 (2004)

Junichi Sakai and Tatsuya Kimura, "Design of a miniature lens for semiconductor laser to single-mode fiber coupling," *J. Quant. Elentron*. Vol.16, pp. 1059 (1980)

J. W. Ogland, "Mirror system for uniform transformation in high power annular laser," *Appl. Opt*., Vol. 17, pp. 2917-2923 (1978)

Kyung-Rok Kim, Selee Chang, and K. Oh, "Refractive microlens on fiber using UV-curable fluorinated acrylate polymer by surface-tension," *IEEE Photonics Technology Letters*, 15, paper 8, pp. 1100-1102 (2003)

L. G. Cohen and M. V. Schneider, "Microlenses for coupling junction lasers to optical fibers," *Appl. Opt*., Vol. 13, pp. 89-94 (1974)

Michael J. hayford et al., "Illumination module user's guide," Optical Research Associates (2003)

M. S. Ho, C. Barrett, J. Paterson, M. Esteghamatian, A. Natansohn, and P. Rochon, *Macromolecules* Vol. 29, pp. 4613 (1996)

N. C. R. Holme, L. Nikolova, P. S. Ramanujam, and S. Hvilsted, *Appl. Phys. Lett.* Vol. 70, pp. 1518 (1997)

P. Rochon, E. Batalla, and A. Natansohn, "Optically induced surface gratings on azoaromatic polymer films.", *Appl. Phys. Lett*. Vol. 66, pp. 136 (1995)

S. Choi, Kyung-Rok Kim and K. Oh, "Interferometric inscription of surface relief gratings on optical fiber using azo polymer film," Appl. Phys. Lett., Vol. 83, pp. 1080 (2003)

Shaoping Bian et al., "Photoinduced surface deformations on azobenzene polymer films", *J. Appl. Phys.*, Vol 86, pp. 4498 (1999)

Shojiro Kawakami, "Light Beam Redistribution using computer generated phase plates," *J. Lightwave Technol.*, Vol. 7, pp.1412-1418 (1989)

S. J. Zilker et al., "Holographic data storage in amorphous polymers", *Adv. Mater.*, Vol. 10, pp. 855 (1998)

T. S. Lee, D. Y. Kim, X. L. Jiang, L. Li, J. Kumar, and S. K. Tripathy, *Macromol. Chem. Phys.* Vol. 198, pp. 2270 (1997)

W. Y. Hung, "Novel design of wide angle single-mode symmetric Y-junctions," *Electron. Lett.*, Vol. 24, pp. 1184-1185 (1988)

Wen-Ching Chang, "A novel low-loss wide angle Y-branch with a diamond-like microprism," IEEE *Photon. Technol. Lett.*, Vol. 11, pp. 683-685 (1999)

X. Wang, L. Li, J. Chen, S. Marturunkakul, J. Kumar, and S. K. Tripathy, *Macromolecules* 30, pp.219 (1997)

X. L. Jiang, L. Li, J. Kumar, D. Y. Kim, and S. K. Tripathy, "Polarization dependent recordings of surface relief gratings on azobenzene containing polymer films.", Appl. Phys. Lett. Vol. 68, pp. 2618 (1996)

X. T. Li et al., "Photoinduced liquid crystal alignment based on a surface relief grating in an assembled cell.", *Appl. Phys. Lett.* Vol. 74, pp. 3791 (1999)

Polymer Thin Films

Edited by Abbass A Hashim

ISBN 978-953-307-059-9
Hard cover, 324 pages
Publisher InTech
Published online 01, April, 2010
Published in print edition April, 2010

This book provides a timely overview of a current state of knowledge of the use of polymer thin film for important technological applications. Polymer thin film book covers the scientific principles and technologies that are necessary to implement the use of polymer electronic device. A wide-ranging and definitive coverage of this emerging field is provided for both academic and practicing scientists. The book is intended to enable readers with a specific background, e.g. polymer nanotechnology, to become acquainted with other specialist aspects of this multidisciplinary field. Part A of the book covers the fundamental of the key aspect related to the development and improvement of polymer thin film technology and part B covers more advanced aspects of the technology are dealt with nano-polymer layer which provide an up-to-date survey of current research directions in the area of polymer thin film and its application skills.

InTech Europe
University Campus STeP Ri
Slavka Krautzeka 83/A
51000 Rijeka, Croatia
Phone: +385 (51) 770 447
Fax: +385 (51) 686 166
www.intechopen.com

InTech China
Unit 405, Office Block, Hotel Equatorial Shanghai
No.65, Yan An Road (West), Shanghai, 200040, China
中国上海市延安西路65号上海国际贵都大饭店办公楼405单元
Phone: +86-21-62489820
Fax: +86-21-62489821

IntechOpen